JOURNAL OF MATERIALS SCIENCE 32 (1997) 207–213

Growth and structure of TiC_xN_y coatings chemically vapour deposited on graphite substrates

S. EROGLU
TUBITAK-Marmara Research Centre, Materials Research Dept. P.K. 21, 41470, Gebze-Kocaeli, Turkey

B. GALLOIS
Stevens Institute of Technology, Department of Materials Science and Engineering, Hoboken, NJ 07030, U.S.A

TiC_xN_y coatings were grown on graphite substrates in a computer-controlled, hot-wall chemical vapour deposition (CVD) reactor, using gas mixtures of $TiCl_4$–CH_4–N_2–H_2 at a total pressure of 10.7 kPa (80 torr) and at a temperature of 1400 K. Growth rate, composition, morphology and crystallographic texture of the TiC_xN_y coatings were investigated as a function of the $CH_4/CH_4 + N_2$ ratio in the range 0–1 at a constant $CH_4 + N_2$ flow rate of 370 standard cubic centimeters per minute (sccm). The $C/C + N$ ratio and growth rate of the TiC_xN_y coatings increased with increasing $CH_4/CH_4 + N_2$ ratio in the gas phase. The compositions of the coatings with $C/C + N$ ratios in the range 0–1 were found to be between the thermodynamic and the kinetic predictions. Morphology and preferred orientation of the coatings were observed to be strongly affected by the $CH_4/CH_4 + N_2$ ratio in the gas phase.

1. Introduction

TiC_xN_y coatings have high hardness, high temperature strength and good corrosion resistance. Because of these properties, they have been used in many areas ranging from cutting tools to nuclear materials. The use of TiC_xN_y coatings is an effective method to improve the surface characteristics of graphite and graphite-based materials. For example, TiC and TiN coatings deposited on graphite substrates as used in fusion reactors reduce surface erosion and help improve plasma impurity control [1, 2].

The chemical vapor deposition (CVD) technique has been widely used to prepare TiC_xN_y coatings from gaseous mixtures of $TiCl_4$–CH_4–N_2–H_2. TiC_xN_y coatings deposited by this technique on metals such as steel [3, 4] or on cemented carbide [5–7] substrates have been the subject of extensive research. There are, however, few publications [8–10] on CVD TiC_xN_y coatings grown on graphite substrates. Eroglu and Gallois [8] investigated residual stresses in TiC_xN_y coatings as a function of coating composition and the graphite substrate material. Textures in these coatings were studied by the same authors [9]. Eroglu and Gallois [10] also synthesized continuously graded TiN/TiC coatings with linear and exponential concentration profiles by varying the $CH_4/CH_4 + N_2$ ratio in the gas phase at constant $CH_4 + N_2$ (175 sccm), $TiCl_4$ (20 sccm) and H_2 (475 sccm) flow rates at 1400 K. This current study was undertaken in order to systematically investigate the influence of the ratio of CH_4 to $CH_4 + N_2$ on the growth rate, composition, morphology and texture of the monolithic TiC_xN_y coatings grown on graphite substrates at a constant $CH_4 + N_2$ flow rate of 370 sccm.

2. Experimental details

The depositions were carried out at 1400 K, a total pressure of 10.7 kPa (80 Torr) and a total flow rate of 670 standard cubic centimeters per minute (sccm) for 75 min in a computer controlled, hot wall CVD reactor described elsewhere [11]. A POCO graphite was used as a substrate. The ratio of CH_4 to $CH_4 + N_2$ was varied from zero to unity at constant $TiCl_4$ (20 sccm) and H_2 (280 sccm) flow rates. The experimental conditions employed for the chemical vapour deposition of the TiC_xN_y coatings are listed in Table I. The deposition of the coatings was conducted in the mass-transport controlled regime [11].

The morphologies were examined by scanning electron microscopy (SEM). The thickness of the coatings was determined from scanning electron micrographs of the cross-sections.

Since the TiC_xN_y lattice parameter variation with composition follows Vegard's law [12], the compositions of the coatings were determined from the lattice

0022–2461

TABLE I Growth rates and lattice constants of TiC_xN_y coatings as a function of CH_4 and N_2 flow rates at a temperature of 1400 K and at a total pressure of 10.7 kPa (80 torr). The total flow rate is constant at 670 sccm and the flow rates of $TiCl_4$ and H_2 are fixed at 20 sccm and 280 sccm, respectively.

Flow rate (sccm)		$CH_4/CH_4 + N_2$ Ratio	Growth rate ($\mu m\ min^{-1}$)	Lattice constant (nm)
CH_4	N_2			
0	370	0	[a]	0.4239
60	310	0.16	0.210 ± 0.02	0.4283
110	260	0.30	0.234 ± 0.003	0.4305
160	210	0.43	0.326 ± 0.007	0.4319
210	160	0.57	0.289 ± 0.008	0.4324
260	110	0.70	0.344 ± 0.003	0.4325
310	60	0.84	0.403 ± 0.008	0.4326
370	0	1.00	0.543 ± 0.06	0.4327

[a] Whiskery deposit.

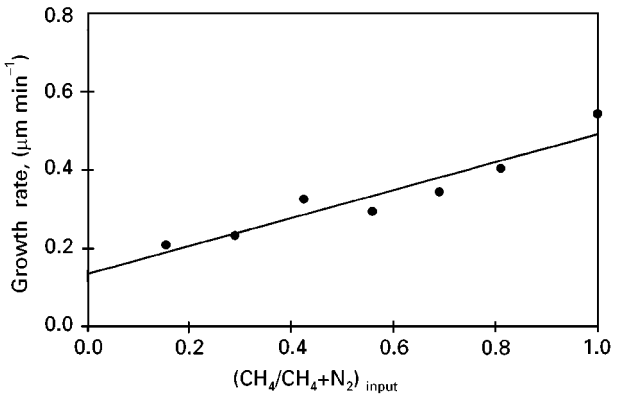

Figure 1 Growth rate of TiC_xN_y coatings as a function of $CH_4/CH_4 + N_2$ ratio at constant flow rates of $CH_4 + N_2$ (370 sccm), $TiCl_4$ (20 sccm) and H_2 (280 sccm) at 1400 K.

parameters measured by the X-ray diffraction technique. It was assumed that x + y is equal to unity. Preferred orientation, expressed in terms of texture coefficients, was also determined by a parafocussing X-ray diffractometer. The details of the lattice constant, composition and texture measurements were described elsewhere [8–10, 13]. The textures of the coatings were also checked by the wide-film Debye–Scherrer X-ray diffraction technique [9].

3. Results and discussion

3.1. Deposition rates of the coatings

Fig. 1 and Table I show the variation of the growth rate of the coatings with the input gas ratio of $CH_4/CH_4 + N_2$. It can be seen that the deposition rate linearly increases with the ratio. Note that no datum is shown for the coating grown at a N_2 flow rate of 370 sccm ($X_{CH_4} = 0$) because of the whiskery appearance of the coating [see Fig. 5a].

A linear increase of the growth rate with the ratio or CH_4 concentration was also observed for the TiC_xN_y coatings grown at a total $CH_4 + N_2$ flow rate of 175 sccm [10] and for TiC coatings [13]. The linear dependence of the growth rate of TiC coatings on the CH_4 concentration was explained by a mass-transport

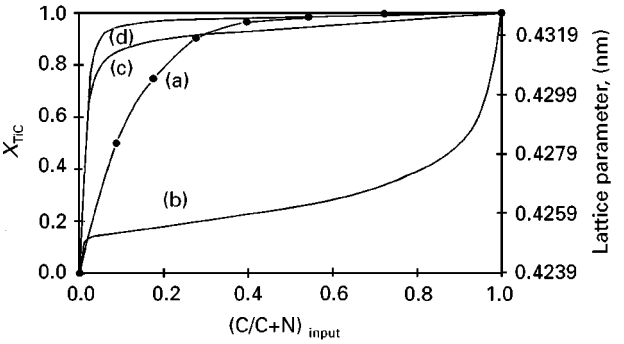

Figure 2 Variations of mole fraction of TiC (X_{TiC}) and lattice constant of the TiC_xN_y coatings with C/C + N ratio in the gas phase: (a) Experimental results; (b), (c), (d) thermodynamic calculations ((b) includes carbon as a solid phase, ideal solution of TiN–TiC; (c) excludes carbon as a solid phase, regular solution of TiN–TiC with $\Omega_{C-N} = -20000\ J\ mol^{-1}$; (d) excludes C as a solid phase, ideal solution of TiN–TiC).

theory, which predicted that the growth rate should be linearly proportional to the input CH_4 gas concentration. Since the depositions of TiC_xN_y coatings were carried out in the mass-transport-limited regime, the mass-transport theory developed for pure TiC coatings can also be applicable to the experimental conditions reported here. The deposition rate can be expressed as [13]

$$\text{rate} \propto (T^{3/2}/P)\,(v/\mu)^{1/2}\,(C_b - C_s) \qquad (1)$$

where T is the deposition temperature, P is the pressure, v is the linear gas velocity, μ is the kinematic viscosity, C_b is the bulk concentration of species in the gas phase, and C_s is the concentration of species on the growth surface. Since the deposition temperature, total pressure and total flow rate were held constant, the growth rate is proportional to the concentration potential above the substrate, assuming no change in kinematic viscosity with gas composition. In the mass-transport controlled regime, the rate of transportation of reactant species to the growth surface is much smaller than the actual consumption rate on the deposition surface. Therefore, it may be assumed that C_b is much larger than C_s. The growth rate of TiC_xN_y then becomes linearly proportional to the bulk reactant concentrations (C_b). Since the flow rates of H_2 and $TiCl_4$ are constant and since the growth rate of pure TiC grown at a CH_4 flow rate of 370 sccm ($X_{CH_4} = 1$) is larger than that of pure TiN at a N_2 flow rate of 370 sccm ($X_{CH_4} = 0$), the deposition rate of TiC_xN_y coatings should increase linearly with the concentration of CH_4 or X_{CH_4}. The experimental results presented here qualitatively agree with the predictions of the mass-transport theory as shown in Fig. 1.

3.2. Compositions of the coatings

Fig. 2 shows the composition of the TiC_xN_y coatings, expressed in terms of the TiC mole fraction in TiC_xN_y, and also as a function of the (C/C + N) ratio in the gas phase. As can be seen from the figure (curve a), the TiC content of the coatings increase rapidly up to a ratio X_{CH_4} equal 0.43 above which it gradually levels off. X-ray diffraction profiles of the high-angle reflections

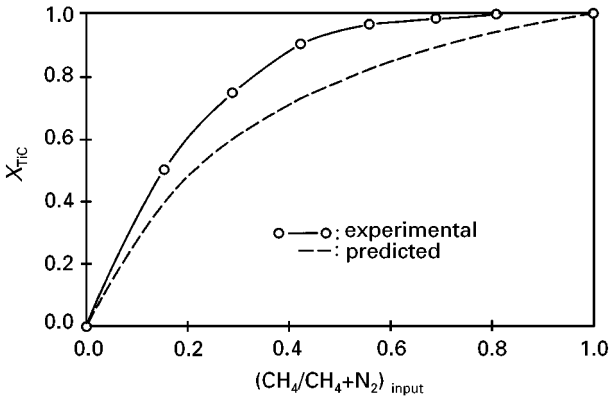

Figure 3 Mole fraction of TiC in TiC_xN_y coatings as a function of $CH_4/CH_4 + N_2$ ratio in the gas phase. The broken line is predicted by a kinetic model.

from the coatings showed sharp lines and well resolved K_{α_1}–K_{α_2} doublets, indicating that the coatings are uniform in composition.

3.2.1. Thermodynamic analysis

The experimental results were compared with the equilibrium thermodynamic compositions determined by the method of minimization of the Gibbs' free energy [10]. The results are summarized in Fig. 2. Curve (b) shows the results of the calculation for an ideal solution when carbon is considered as a possible solid phase. The equilibrium solid phase consists of TiC–TiN and free carbon. The agreement with the experimental data (curve (a)) is poor. X-ray diffraction, Auger electron spectroscopy and microstructural studies reveal, however, the absence of free carbon in the deposit [13]. This result implies that kinetic limitations exist which prevent the formation of free carbon. Therefore, in subsequent calculations it was assumed that free carbon was not formed. Curves (c) and (d) were calculated for a regular solution with $\Omega_{C-N} = -20000\ J\ mol^{-1}$ and for an ideal solution, respectively. The shapes of curves (c) and (d) agree qualitatively with the experimental data. At low $CH_4/CH_4 + N_2$ ratios, (less than 0.25), the agreement is poorer compared to higher ratios.

3.2.2. Kinetic analysis

If we assume that growth rate of titanium carbonitride (TiC_xN_y) is the sum of the deposition rates of TiC (G_{TiC}) and TiN (G_{TiN}), then the solid compositions of the carbonitrides can be expressed as [10]

$$X_{TiC} = G_{TiC}/(G_{TiC} + G_{TiN}) = G^*_{TiC}\,X_{CH_4}/(G^*_{TiC}\,X_{CH_4} + G^*_{TiN}\,X_{N_2}) \quad (2)$$

where X_{TiC} is the mole fraction of TiC in titanium carbonitride, G^*_{TiC} is the growth rate of TiC at a CH_4 flow rate of 370 sccm ($X_{CH_4} = 1$), G^*_{TiN} is the growth rate of TiN at a N_2 flow rate of 370 sccm ($X_{CH_4} = 0$ or $X_{N_2} = 1$). The least square fit to the kinetic data of Table I yields constant values of G^*_{TiC} and G^*_{TiN} of 0.493 and 0.134 μm min^{-1}, respectively. The solid compositions as a function of X_{CH_4} are then obtained from Equation 2 using the constants and the results are plotted in Fig. 3. The predicted compositions are found to be lower in TiC content, but show a similar trend to that of experimental results.

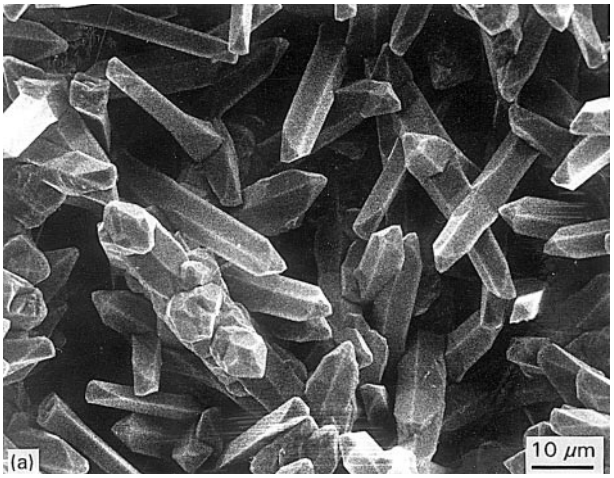

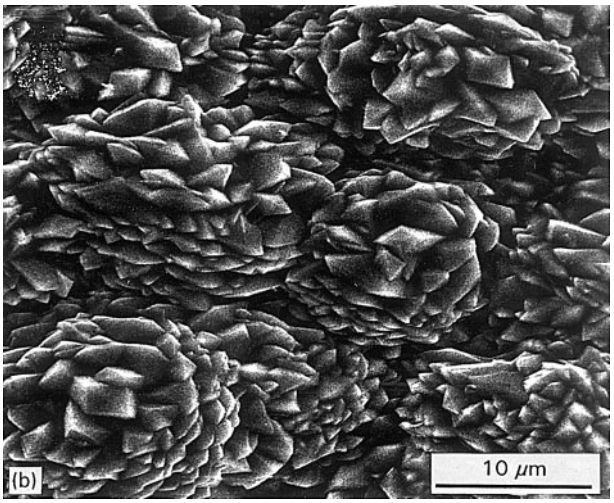

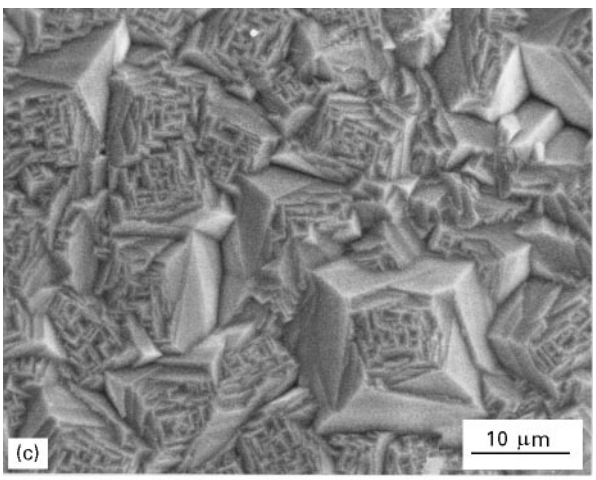

Figure 4 Surface morphologies of the coatings grown at $CH_4/CH_4 + N_2$ ratios of (a) 0, (b) 0.16 and (c) 0.84.

3.3. Morphology of the coatings

The development of the morphologies of the coatings are shown in Figs 4 and 5 for increasing values of the

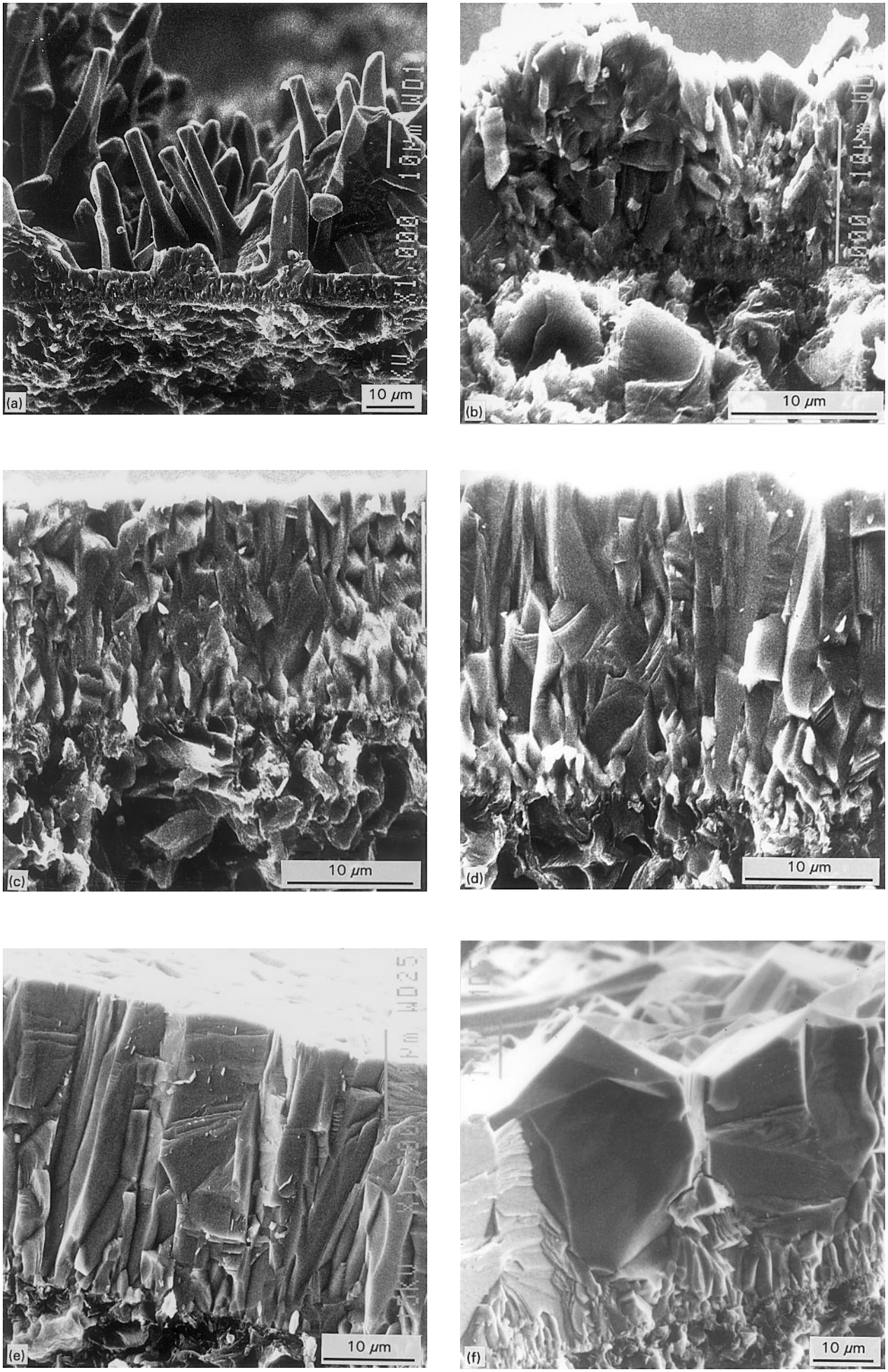

Figure 5 Cross-sectional views of the coatings grown at $CH_4/CH_4 + N_2$ ratios of (a) 0, (b) 0.16, (c) 0.3, (d) 0.43, (e) 0.84 and (f) 1.

ratio X_{CH_4}. Surface morphologies range from whiskers through nodular and pyramidal surface features to highly faceted large grains. Fig. 4a shows that the surface appearance of a pure TiN coating consists of whiskers. The whisker directions appear to be random with respect to the substrate normal. No branching or kinking of the whiskers is observed. The coating grown at a ratio of 0.16 has a nodular surface morphology seen in Fig. 4b which consists of small grains of the order of 1 or 2 μm. Rose-like features are observed in the coating grown at a ratio of 0.84 as shown in Fig. 4c.

The cross-sectional view of a pure TiN coating seen in Fig. 5a reveals whiskers infiltrated by a 6 μm-thick layer of deposit on the substrate surface, suggesting that the whisker formation started before the deposition of the layer. The fractured surface of the coating grown at a ratio of 0.16 exhibits a porous structure as seen in Fig. 5b. The deposition conducted at a ratio of 0.3 shows a cross section with less porosity than the previous sample (Fig. 5c). The fractured cross section of the deposit grown at 0.43 has typical columnar grains originating from small grains near the substrate (Fig. 5d). The cross-sectional view of the coating deposited at 0.84 reveals dense and large columnar grains (Fig. 5e). A fractured surface of the pure TiC coating seen in Fig. 5f is characterized by strongly faceted large columnar grains. The facets are identified to be (111) planes as deduced from the angle of about 108 degrees between the facets. The diameter of the grain in the middle of the micrograph increases with increasing coating thickness until it impinges another abnormal grain which is shown in the right side of the micrograph. The increase in diameter indicates that the grain grows at the expense of other grains. When the abnormal grain impinges into another abnormal one, the increase in diameter ceases and it does not change with the thickness as shown in Fig. 5f.

These observations agree well with the models developed by Ling and Anderson [14]. They reported that the grains that have low solid–vapour interfacial energies tend to grow abnormally and that the driving force for abnormal growth is the decrease in the grain boundary area. It was also reported that once impingement occurs, the grain expansion or the increase in diameter ceases because none of the abnormal grains has any advantage over the others.

3.4. Texture of the coatings

X-ray diffraction profiles revealed that almost all the coatings exhibited X-ray peak intensities which deviated from those observed in random powder samples. The coatings have a preferred orientation of a particular set of crystal planes parallel to the substrate, producing a fibre texture with the fibre axis parallel to the growth direction. The results of preferred orientation studies are summarized in Table II. As seen from the table, the coatings grown at low X_{CH_4} ratios (0 and 0.16) exhibit a slight preferred orientation in the ⟨110⟩ direction. This result is expected from the coatings with grains randomly oriented as shown in Fig. 5(a, b). A strong ⟨110⟩ texture develops in the coating when the X_{CH_4} ratio is 0.3. At a ratio of 0.43, the texture changes to a ⟨100⟩ orientation. The coating deposited at a ratio of 0.57 is preferentially oriented in ⟨110⟩ direction. The ⟨110⟩ orientation observed for the coating prepared at 0.7 is much stronger compared to previous coating. The columnar grains of the coating (see Fig. 5e) grown at 0.84 are mostly oriented in the ⟨100⟩ direction. A pure TiC coating shows a ⟨110⟩ texture.

TABLE II Variation of texture coefficients of the (111), (200), (220) and (113) reflections from TiC_xN_y coatings with the input gas composition.

$CH_4/CH_4 + N_2$ Ratio	Texture coefficient			
	(111)	(200)	(220)	(113)
0.00	0.68	0.73	1.34	1.25
0.16	0.74	0.70	1.31	1.25
0.30	0.18	0.15	3.24	0.43
0.43	0.00	2.69	0.26	1.05
0.57	0.00	1.57	2.25	0.18
0.70	0.00	0.07	3.90	0.03
0.84	0.00	3.73	0.22	0.05
1.00	0.12	0.89	1.86	1.19

To summarize the texture studies, the coatings have either ⟨100⟩ or ⟨110⟩ orientation and no correlation between preferred orientation and input gas composition is found for the experimental conditions investigated here. The textures of the coatings are, however, greatly affected by the input methane concentration as seen in Table II. It should be noted that no reflection from the (111) crystal planes are obtained from the coatings deposited at X_{CH_4} ratios in the range 0.43–0.84. The source of the development of textures might be related to the preferential attachment of gaseous species on crystal planes, thus inhibiting or promoting the growth of certain crystallographic planes.

The textures studies performed by conventional X-ray diffractometer techniques were checked by a wide-film Debye–Scherrer X-ray diffraction technique described elsewhere [9]. Fig. 6(a–d) show the X-ray diffraction patterns of the coatings grown at X_{CH_4} ratios of 0.16, 0.30, 0.84 and 1. The pattern of the coating deposited at 0.16 consists of continuous diffraction rings seen in Fig. 6a, indicating that no strong texture exists in the coating. Fig. 6b reveals that a ⟨110⟩ preferred orientation is present in the coating grown at 0.3 as characterized by a high intensity of the (220) diffraction ring. The coating grown at 0.84 exhibits discontinuous rings with non-uniform intensities (Fig. 6c). The (200) reflection from this coating has a much higher intensity at its central position in the form of short arc, which indicates that very sharp ⟨100⟩ orientation exists in the coating. Notice that no reflection from the (111) crystal plane is seen in the diffraction pattern. The X-ray diffraction pattern of pure TiC coating is comprised of spotty rings because of large grains. The pattern also contains a slight ⟨110⟩ texture signalled by a higher intensity near the equatorial plane of the diffraction pattern. The results obtained by the film technique are found to be in good agreement with those of the conventional diffractometer.

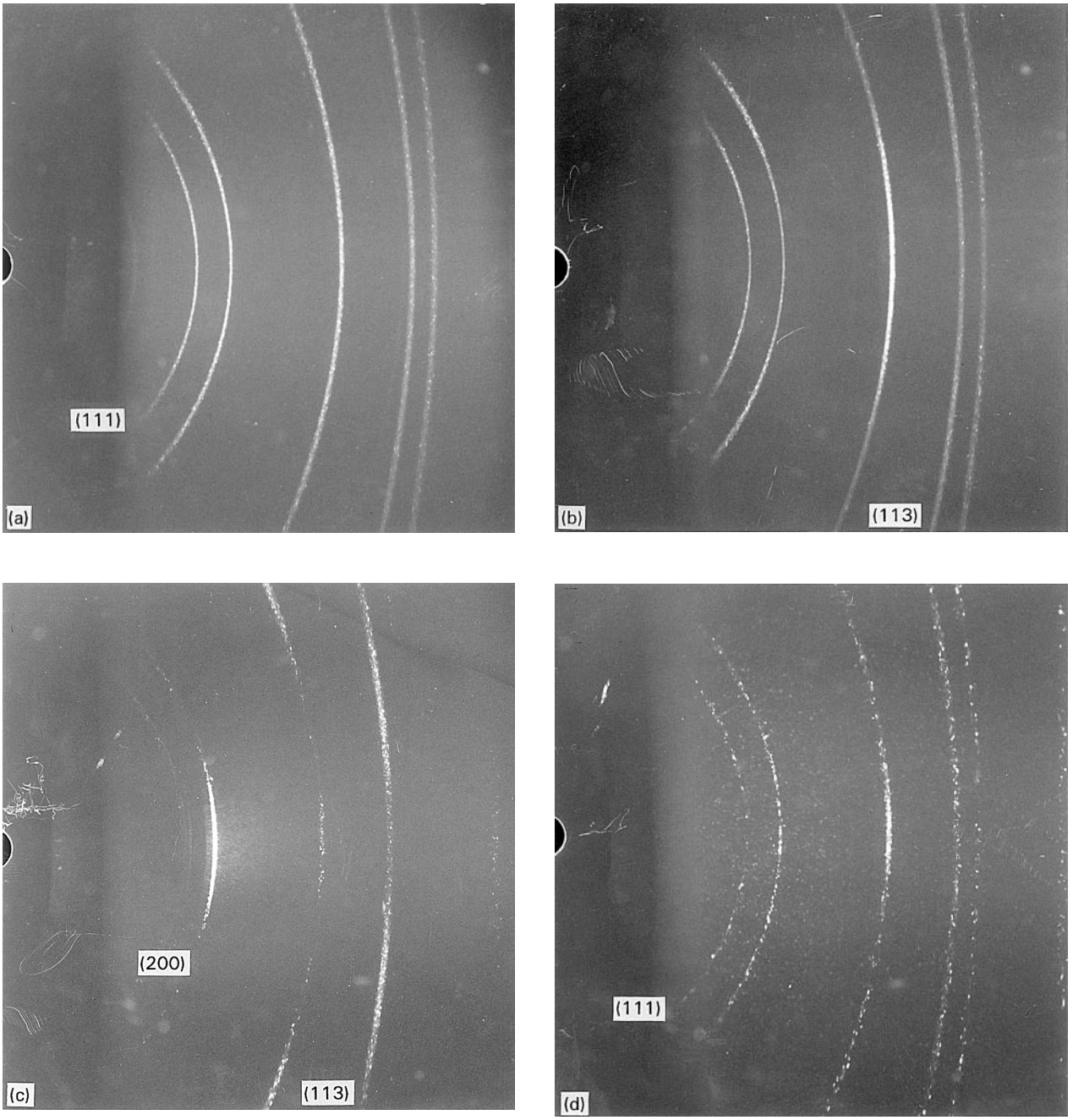

Figure 6 Wide-film Debye–Scherrer X-ray diffraction patterns of the coatings grown at $CH_4/CH_4 + N_2$ ratios of (a) 0.16, (b) 0.30, (c) 0.84 and (d) 1.

4. Conclusions

TiC_xN_y coatings with a C/C + N ratio in the range 0–1 were deposited by the CVD technique by varying the ratio of CH_4 to $CH_4 + N_2$ at a constant $CH_4 + N_2$ flow rate of 370 sccm in the mass-transport limited regime at 1400 K. The growth rate of the coatings increased linearly with the $CH_4/CH_4 + N_2$ ratio, in agreement with the mass-transport theory. The TiC content in the TiC_xN_y coatings also increased with the input CH_4 concentration. The experimental compositions of the coatings were found to be between those of kinetic and thermodynamic predictions. The coatings grown at X_{CH_4} ratios of 0, 0.13 and 1 showed rough morphologies, whereas TiC_xN_y coatings at ratios between 0.13 and 1 exhibited relatively smoother morphologies and sharper preferred orientations which varied between the $\langle 100 \rangle$ and $\langle 110 \rangle$ directions with the input CH_4 concentration.

Acknowledgements

The authors gratefully acknowledge the partial support of the Army Research Office, Division of Materials Science, under contract DAAG29–85–K–0124, and the New Jersey Advanced Technology Centre for Surface Engineered Materials. S. Eroglu was partially supported by the Ministry of Education of the Republic of Turkey.

References

1. M. KOMINSKY, R. NIELSEN and P. ZSCHACK, *J. Vac. Sci. Tech.* **20** (1982) 1304.

2. K. SATO, M. MOHRI and T. YAMASHINA, *J. Nuclear Materials* **103 & 104** (1981) 273.
3. H. O. PIERSON, *Thin Solid Films* **40** (1977) 41.
4. G. F. WAKEFIELD and J. A. BLOOM, in Proceedings of the 3rd International Conference on Chemical Vapor Deposition, Edited by F. A. Glaski (American Nuclear Society, Hinsdale, Illinois, 1972) p. 397.
5. J. S. CHO, S. W. NAM and J. S. CHUN, *J. Mater. Sci.* **17** (1982) 2495.
6. W. P. SUN, D. J. CHENG and M. H. HON, *J. Crystal Growth* **71** (1985) 787.
7. C. W. LEE and J. S. CHUN, in Proceedings of the 8th International Conference on Chemical Vapor Deposition, edited by J. M. Blocher, G. E. Vuillard and G. Wahl (Electrochemical Society, Pennington, NJ, 1981) p. 563.
8. S. EROGLU and B. GALLOIS, *Journal de Physique IV* **3** (1993) 155.
9. *Idem. ibid.* **3** (1993) 177.
10. *Idem. Surf. Coat. Technol.* **49** (1991) 275.
11. J. S. PAIK, Ph.D. Thesis, Stevens Institute of Technology, Hoboken, New Jersey (1991).
12. P. DUWEZ and P. ODELL, *J. Electrochem. Soc.* **97** (1950) 299.
13. S. EROGLU and B. GALLOIS, *J. Mater. Sci.* **30** (1995) 1754.
14. S. LING and M. P. ANDERSON, *J. Electronic Mater.* **17** (1988) 459.

Received 28 March 1995
and accepted 15 December 1995